Surface electronic properties of Fe(100)

A. M. Turner and J. L. Erskine
Department of Physics, University of Texas, Austin, Texas 78712
(Received 15 May 1984; revised manuscript received 27 July 1984)

The band dispersion and magnetic exchange splitting of surface states and surface resonances on Fe(100) are extensively studied using angle-resolved photoemission spectroscopy. Surface-sensitive features in photoemission spectra are observed along the $\bar{\Delta}$, $\bar{\Sigma}$, and $\bar{Y}$ directions of the two-dimensional Brillouin zone. Polarized light from the Tantalus storage ring is used to separate excitations from even- and odd-symmetry initial states along the $\bar{\Delta}$ and $\bar{\Sigma}$ directions. Features identified as surface states are analyzed in relation to bulk electronic states of the same symmetry and spin projected onto the two-dimensional Brillouin zone. Binding energies and dispersion of the features identified as surface states are in good agreement with recent slab calculations over most of the two-dimensional Brillouin zone probed by the experiments. Several surface states and resonances are observed which do not appear to have been predicted theoretically. The results reported in this paper represent an attempt to provide a comprehensive experimental evaluation of the ability of current generation slab calculations to correctly predict surface electronic properties of magnetic surfaces.

I. INTRODUCTION

Recent progress in calculational techniques has made possible detailed and physically meaningful theoretical investigations of bulk[1–6] and surface[7–12] electronic properties of magnetic metals. The importance of being able to accurately predict electronic properties is obvious. Electronic structure provides the basis for explaining fundamental physical phenomena of bulk matter such as magnetic properties, heat capacity, and optical and transport properties. Similarly, surface phenomena such as surface magnetism, chemisorption, surface reconstruction, and catalysis will eventually be more thoroughly understood in terms of electronic structure intrinsic to surfaces. Calculations based on thin magnetic crystals, in particular, have been stimulated by the possible role of surface phenomena in reconciling differences between photoemission experiments and self-consistent band-structure calculations of ground-state electronic structure.[13] Other experiments involving magnetic thin films have raised important questions regarding magnetic dead layers at surfaces,[14,15] and new experiments which resolve spin polarization have also stimulated work in this area.[16,17]

Self-consistent all-electron calculations are only feasible for very thin films and for simple metals having a small number of electrons. However, recent calculations[9–11] have shown that the localized nature of $3d$ states in transition metals permits rapid convergence of the charge density in thin films to the bulk value. This result suggests that self-consistent slab calculations of magnetic thin films having only a few layers (i.e., 7 to 9) should provide accurate and meaningful results for surface electronic properties.

Thin-film calculations for magnetic metals have predicted several interesting new phenomena, and have also provided a broad range of results which can be subjected to fairly thorough experimental tests. For example, enhancement of the surface-layer spin magnetic moment (over the bulk value) of both Fe(100) (Ref. 10) and Ni(100) (Ref. 9) have been predicted. The exchange splitting of magnetic surface states is also predicted to differ significantly from the average bulk values,[1–6] and a large number of magnetic surface states and surface resonances are predicted throughout the two-dimensional Brillouin zones of high-symmetry crystal faces of Fe (Refs. 7–12) and Ni (Refs. 7–9) surfaces. The surface-state predictions, in particular, can be subjected to direct experimental analysis. It would appear that a careful test of the surface-state predictions would constitute a check of the accuracy of the calculations and, in some respects, would also test how well rapid convergence of the charge density with layer thickness implies meaningful surface predictions.

In this paper we present experimental results which constitute a rigorous and fairly comprehensive test of predictions based on thin-film calculations for ferromagnetic Fe surfaces. We have used angle-resolved photoemission to study the surface electronic properties of the Fe(100) surface. Our experiments were conducted with polarized light from the Tantalus storage ring (University of Wisconsin—Stoughton) which permitted initial states of even and odd symmetry to be separated; however, our experiments did not distinguish spin, and conclusions we draw regarding magnetic subbands are based on results of slab calculations.

It is now fairly well established that correlation effects play a significant role in reconciling calculated ground-state energies with the excitation energies of bulk electronic states measured by photoemission.[18,19] These effects appear to be particularly important in d-band metals, especially Ni, and, although they have not been identified in relation to surface phenomena, correlation effects undoubtedly play some role. In this paper, all such effects are neglected, and we adopt the point of view that our

binding-energy measurements reflect the calculated ground-state properties of the magnetic surface. There is some justification for this point of view. We have recently completed a comprehensive experimental investigation of the bulk electronic properties of Fe.[20] This work has shown that correlation effects, which account for 30% differences between excitation energies and calculated ground-state energies in Ni, are significantly smaller in Fe, amounting to, at most, a 10% effect. We assume that the errors associated with directly comparing our excitation energies determined from photoemission and the ground-state calculations for surface states are of the same order, i.e., 10%. The fact that we found excellent agreement between the calculated ground-state energies and our photoemission studies of the bulk band structure of Fe (i.e., correlation effects are small) suggests that our choice of Fe for testing slab calculations for magnetic metals is a good one.

The results presented in this paper provide fairly convincing evidence that the thin-film calculations for Fe, which have been carried out using several different techniques, yield surface-state bands which are generally in good agreement with experiments. Apparently, accurate calculations based on very thin films provide meaningful insight into physical phenomena at magnetic metal surfaces.

II. EXPERIMENTAL CONSIDERATIONS

Our experiments were conducted at the Synchrotron Radiation Center in Stoughton, Wisconsin, using the stainless-steel Seya Namioka monochromator, and an angle-resolving photoelectron spectrometer which has been described in detail elsewhere.[21,22] The spectrometer incorporates low-energy electron diffraction (LEED) and Auger-electron spectroscopy (AES) for surface characterization, and the angle-resolving electron-energy analyzer is capable of operating at the high angular and energy resolution required for mapping surface and bulk electronic structure. The experiments reported in this paper were conducted using a $\pm 1.2°$ angular resolution and an energy resolution (analyzer plus monochromator) of 100 meV.

Our Fe crystal was obtained from Leico, Inc. and was aligned, cut, polished, and cleaned using standard techniques as discussed previously.[23] In order to study surface states and surface resonances on Fe surfaces, it is necessary to obtain particularly clean and well-ordered surfaces. Based on Auger analysis, our "clean"-surface data corresponds to surfaces having less than $\frac{1}{10}$ of a monolayer (ML) of oxygen, and no other detectable surface impurities. Residual surface oxygen ($\frac{1}{10}$ ML) produced an O 503-eV Auger peak less than one-fifth the intensity of the Fe 550-eV peak. LEED analysis showed that the clean Fe surfaces were well ordered.

The sample manipulator of our spectrometer allows translational motion to access LEED-Auger optics, as well as the angle-resolving electron optics. Figure 1 illustrates the two rotational degrees of freedom of the sample (θ_I and ϕ_I) and defines the parameters used in the paper to specify the light polarization, the incident angle of synchrotron radiation, and the electron-emission angles. Two

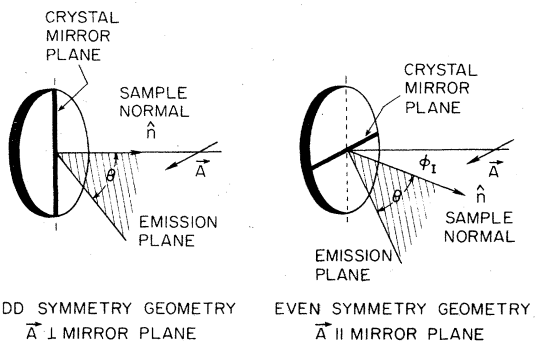

FIG. 1. Sample geometry: θ_I and ϕ_I define angle of incidence. Crystal mirror plane is parallel to manipulator axis. Emission angles are measured from sample normal.

different sample orientations were used, corresponding to an azimuthal alignment of the crystal having the [010] or [1$\bar{1}$0] mirror plane parallel to the polarization vector. When $\phi_I = 0°$, θ_I determines the angle of incidence of pure s-polarized light. In this configuration, the $\vec{A}$ vector is parallel to the mirror plane of the crystal, and there is no component of $\vec{A}$ perpendicular to the surface. When $\theta_I = 0°$, ϕ_I specifies the angle of incidence of mixed s plus p polarization which determines the ratio of $\vec{A}$ components parallel and perpendicular to the surface.

The analyzer is mounted on a double-axis goniometer, which permits access to any emission direction characterized by the two angles θ and ϕ measured from the sample normal and the crystal mirror plane. Any point of the two-dimensional Brillouin zone is accessible by suitable choice of θ, ϕ, and photon energy.

III. BULK AND SURFACE PHOTOEMISSION

Electrons detected in a photoemission experiment can originate directly from bulk initial states, initial states associated with surface atoms, or from various elastic and inelastic scattering processes. Fortunately, there are established techniques which permit assignment of structure in photoemission spectra to bulk initial states, surface states and resonances, and the various loss mechanisms associated with electronic excitations in solids. A comprehensive and accurate description of the bulk electronic states in a solid is one of the most important prerequisites for studying surface states. In this section we summarize some of the results of our recent experiments which have established the bulk electronic structure of Fe,[20] and describe the principal methods we have used to identify structure in photoemission spectra as having originated from surface states.

The fundamental difference between bulk and surface electronic states is that bulk states occupy three-dimensional space, and surface states, by definition, are localized at the surface and are therefore constrained to two dimensions. This implies that band descriptions of extended states in solids require three-dimensional $\vec{k}$ vectors for bulk states, but only two-dimensional $\vec{k}$ vectors

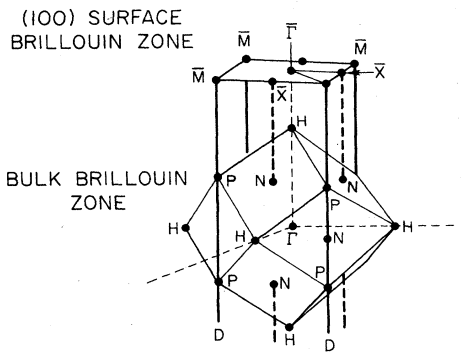

FIG. 2. Illustration of bulk (three-dimensional) and surface (two-dimensional) Brillouin zones for a bcc lattice.

for surface states, and, correspondingly, three- and two-dimensional Brillouin zones. Figure 2 illustrates the three-dimensional Brillouin zone for a bcc lattice and the corresponding two-dimensional Brillouin zone for a (100) crystal face, along with the various high-symmetry points in the two zones.

When photoemission occurs, an electron is excited from an occupied state below the Fermi level into a final state above the vacuum level. In a direct-excitation process, energy conservation requires that the energy difference between the initial and final states be equal to the photon energy:

$$E_f - E_i = \hbar\omega \ . \tag{1}$$

A large number of experiments have now established that the vacuum-crystal interface permits conservation of electron wave vector $\vec{k}$ parallel to the surface modulo a surface reciprocal-lattice vector $\vec{G}$. Therefore,

$$\vec{k}_{\parallel\,\text{outside}} = \vec{k}_{\parallel\,\text{inside}} \pm \vec{G} \ , \tag{2}$$

$$\vec{k}_{\parallel\,\text{outside}} = \left[\frac{2m}{\hbar^2} E_k\right]^{1/2} \sin\theta \ . \tag{3}$$

In these expressions, $\vec{k}_{\parallel}$ refers to the component of wave vector parallel to the surface, E_k is the kinetic energy of the emitted electron, and θ is the emission angle measured from the surface normal. These expressions apply to transitions from bulk states as well as surface states, and form the basis for the analysis of photoemission spectra using the direct-transition model.[24,25] The final state can be a bulk band state or an evanescent LEED state; the LEED final state is usually the case for emission from surface states and surface resonances.

Referring to Fig. 2, it is clear that points corresponding to given values of $\vec{k}_{\parallel}$ in the two-dimensional Brillouin zone also correspond to lines in the three-dimensional Brillouin zone. For example, the $\bar{M}$ point of the two-dimensional Brillouin zone corresponds to a line through the three-dimensional zone which intersects the high-symmetry points labeled P and N. One problem in characterizing surface states by photoemission is to ensure that features in a photoemission spectrum, believed to be associated with surface states, originate from initial states in the two-dimensional Brillouin zone, rather than from states having the same $\vec{k}_{\parallel}$ but originating from the three-dimensional Brillouin zone.

There are three tests which can be applied to photoemission features which permit discrimination between bulk and surface-state features. These tests are summarized here, and have been used to test all of the features we attribute, in this paper, to surface states and surface resonances. The first test simply involves checking to see that adsorbed molecules or surface disorder produced by ion bombardment affects the state as viewed by photoemission. Most surface states are strongly affected by the surface conditions. In the present study, small doses of oxygen and low coverages of sulfur obtained by high-temperature annealing were found to be very effective in quenching surface states. In addition, surface disorder induced by gentle ion bombardment was found to effectively quench the surface states.

The second test for a surface state is to check for the two-dimensional character of the state. If the photon energy and emission angle are changed in such a way as to keep $(E_k)^{1/2}\sin\theta$ constant, then $\vec{k}_{\parallel}$ is constant, and the same point in the two-dimensional Brillouin zone is probed by photoemission. Because bulk photoemission involves transition to a bulk final state, changing the photon energy necessarily results in emission from a different portion of the three-dimensional Brillouin zone even though $\vec{k}_{\parallel}$ is the same. If there is any dispersion of the bulk initial state with $\vec{k}_{\perp}$, the binding energy of the peak will shift, indicating it is a bulk state. If the binding energy does not depend on photon energy for a fixed value of $\vec{k}_{\parallel}$, the state is two dimensional and therefore is very likely to be associated with a surface state or surface resonance.

The third criterion for a surface state is that it must lie in a gap of the bulk bands projected onto the two-dimensional Brillouin zone. The projections must be made for each spin in a ferromagnetic metal, and for states having even or odd symmetry with respect to the emission plane (which is assumed to be a mirror plane of the crystal). In some instances, surface resonances occur. These are states which do not lie in gaps, but rather in the projected bulk band continuum and satisfy the other two criteria outlined above, i.e., they exhibit two-dimensional dispersion with $\vec{k}_{\parallel}$ and are very sensitive to surface conditions.

Application of the first two criteria for surface states can be accomplished directly by comparison of photoemission energy-distribution curves (EDC's) obtained at fixed values of $\vec{k}_{\parallel}$ but different photon energies for clean and adsorbate-coated surfaces. Computations are required to verify the third criterion. We have used a computer program which calculates bulk bands for ferromagnetic Fe to project bulk bands at five points along each of the three high-symmetry lines of the two-dimensional Brillouin zone: $\bar{\Gamma}$–$\bar{X}$, $\bar{\Gamma}$–$\bar{M}$, and $\bar{M}$–$\bar{X}$. To obtain high accuracy in our projected bands, we have used critical-point binding energies obtained from photoemission[20] (which agree very well with recent calculations) to make small corrections of calculated bulk bands projected onto

the two-dimensional Brillouin zone. Our experimental data showing surface-state peaks are plotted as points (representing binding energies at various values of $\vec{k}_{||}$) on these projections which represent experimentally verified projections of the bulk bands onto the two-dimensional Brillouin zone.

One final point worth mentioning before discussing our experimental results is related to the choice of photon energies, and how this choice affects analysis of the photoemission data. In our study of the bulk band structure of ferromagnetic Fe we found that surface processes dominated photoemission from the (100) crystal face for certain photon energies and emission directions. Emission normal to the Fe(100) surface ($\vec{k}_{||}=0$) probes bulk initial states along the Δ line of the three-dimensional Brillouin zone which extends from the zone center Γ to the zone edge H. Selection rules govern allowed dipole-interband transitions.[26,27] Along the Δ line, transitions are allowed from Δ_1- and Δ_5-symmetry initial-state bands into Δ_1-symmetry final-state bands. Examination of the calculated band structure of ferromagnetic Fe (Ref. 1) reveals that the two Δ_1-symmetry subbands which lie above E_F change to Δ_5 symmetry at H, the zone edge. This implies that there are no final states of Δ_1 symmetry in that part of the three-dimensional Brillouin zone accessible with certain photon energies (i.e., in a range from about 15 to 30 eV). A gap in the symmetry-allowed Δ_1 final-state band does not occur for the (110) crystal face (Σ line) or the (111) crystal face the (Λ line) for bcc lattices, and, in general, we found that bulk transitions dominate the photoemission spectra of Fe for emission along these directions. The surface sensitivity of Fe(100) in the photon-energy range from approximately 15 to 30 eV is a consequence of the absence of a Δ_1-symmetry final-state band. We have used this photon-energy range in order to suppress bulk emission in our studies of the surface electronic properties of Fe(100).

Symmetry rules also apply to surface-state emission and form the basis for separating states according to symmetry and spin. Dipole transitions preserve the spin quantum number, and the symmetry of an initial state can be directly determined from photoemission if polarized light is used to excite the dipole transition. In our experiments, photoelectrons were detected in a mirror plane of the crystal, and the electric field vector was chosen to lie either parallel or perpendicular to the mirror plane. The final state detected by photoemission is always an even-symmetry state (reflection symmetry in the mirror plane), and the initial state, which is connected to the final state by the dipole matrix element, is either even ($\vec{A}_{||}$ mirror plane) or odd ($\vec{A}_{\perp}$ mirror plane), depending on which configuration is used. This property explains our use of even and odd symmetry to specify the states which are probed by a particular experimental configuration. Figure 3 illustrates the two basic configurations used in our experiments to probe even- and odd-symmetry initial states of the two-dimensional Brillouin zone.

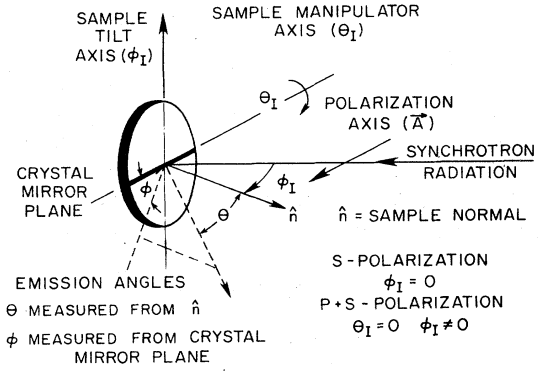

FIG. 3. Illustration of the even- and odd-symmetry geometries used in the experiments.

IV. EXPERIMENTAL RESULTS

There are three high-symmetry lines in the two-dimensional Brillouin zone of Fe(100), shown in Fig. 2, which we have studied. These lines are designated the $\bar{\Sigma}$ line which extends from $\bar{\Gamma}$ to $\bar{M}$, the $\bar{\Delta}$ line which extends from $\bar{\Gamma}$ to $\bar{X}$, and the $\bar{Y}$ line which extends from $\bar{M}$ to $\bar{X}$. Even and odd states were distinguished experimentally along the $\bar{\Sigma}$ and $\bar{\Delta}$ lines by appropriate choice of the $\vec{A}$ vector in relation to the symmetry axis (refer to Fig. 3). The $\bar{Y}$ line presents a more complicated situation in rela-

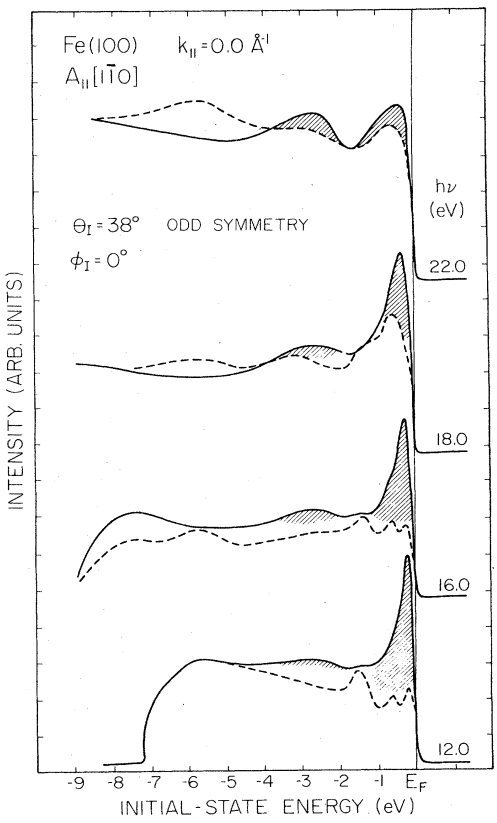

FIG. 4. Normal-emission EDC's taken in odd-symmetry geometry. Solid lines, clean surface; dashed lines, after 0.3 L oxygen dose. Hatched regions are from surface-state emission. Small peaks in dashed curves are from bulk transitions.

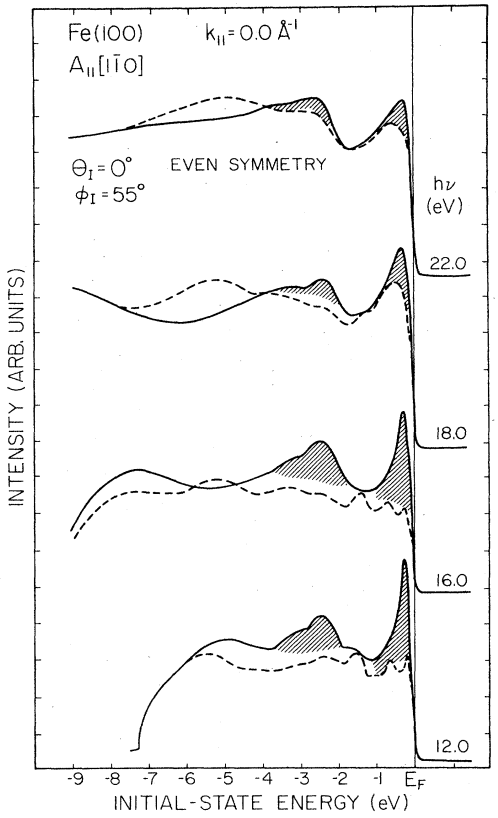

FIG. 5. Normal-emission EDC's taken in even-symmetry geometry. Solid lines, clean surface; dashed lines, after 0.3 L oxygen dose. Hatched regions are from surface-state emission.

tion to projecting the bulk bands because they do not separate according to even and odd symmetry. Results for each of these are discussed separately in the following subsections.

A. The $\bar{\Sigma}$ line

We investigated the behavior of bulk and surface emission features of Fe(100) along the $\bar{\Sigma}$ line of the two-dimensional Brillouin zone using the two configurations illustrated in Fig. 3. In both configurations, the [1$\bar{1}$0]-symmetry axis of the crystal is parallel to the $\vec{A}$ vector. In one case, the angle of incidence was 38° ($\theta_I=38°$ and $\phi_I=0°$; refer to Figs. 1 and 3), and electrons were detected in the plane of incidence, parallel to the crystal [110] direction. In this configuration, the light is pure s polarized, and the emission plane is perpendicular to $\vec{A}$; therefore, only odd-symmetry surface states are probed. In the other configuration, the angle of incidence was 55° ($\theta_I=0°$ and $\phi_I=55°$), and electrons were detected in the [1$\bar{1}$0] direction. In this configuration the light is mixed s and p polarization, and the emission plane is parallel to $\vec{A}$; therefore, only even-symmetry surface states are probed.

Figures 4 and 5 display electron energy-distribution curves for these two configurations at the center of the two-dimensional Brillouin zone for four photon energies. EDC's for clean surfaces are represented by solid lines, and dashed lines illustrate the effect of adsorbing 0.3 L (1 L=1 langmuir=1×10^{-6} Torr sec) of oxygen. These two figures show that there are two prominent odd-symmetry features at $\bar{\Gamma}$, with binding energies of approximately 0.3 and 2.8 eV, and three even-symmetry features, with binding energies of approximately 0.25, 2.5, and 3.8 eV. The binding energies of these structures in the clean EDC's do not change with photon energy, and they are clearly very sensitive to submonolayer oxygen coverages.

We have studied the dispersion of these even- and odd-symmetry surface-sensitive features along the $\bar{\Sigma}$ line in the two configurations described above. Figure 6 displays representative EDC's for odd- and even-symmetry surface-state features at four points along the $\bar{\Sigma}$ line. We have chosen to display odd- and even-symmetry EDC's at two photon energies and at a given point along the $\bar{\Sigma}$ line in each panel of the figure to help illustrate the differences in EDC's associated with the two emission geometries. It is easier to note the differences between the even- and odd-symmetry states when they are compared at each value of $\vec{k}_{\parallel}$.

We have plotted the binding energy of even- and odd-symmetry peaks as a function of $\vec{k}_{\parallel}$ over projections of even- and odd-symmetry bulk bands onto the two-dimensional Brillouin zone. Figure 7 illustrates an intermediate step in projecting the bulk bands. We first compute the bulk energy bands along the line in the three-dimensional Brillouin zone which corresponds to a specific value of $\vec{k}_{\parallel}$ in the two-dimensional zone. The bands shown in Fig. 7 correspond to the rod under $\vec{k}_{\parallel}=0.75$ Å^{-1}, a point halfway between $\bar{\Gamma}$ and $\bar{M}$. In some cases we have used the critical-point binding energies of bulk bands we have determined by photoemission[20] to adjust calculated bands to provide accurate projections.

Figure 8 displays the peak locations of even-symmetry ($\bar{\Sigma}_1$) peaks along the $\bar{\Sigma}$ line plotted over projections of majority- and minority-spin even-symmetry bulk bands. Our experiments do not distinguish spin; therefore, the surface-state locations are plotted in both majority- and minority-spin projections. However, we have shown two types of points (denoted by solid and open rectangles) to distinguish the correct points for each panel (i.e., data points which we think correspond to the correct spin subband). The bold solid lines on each panel illustrate the position of surface states and resonances predicted by self-consistent slab calculations.[10,11]

Figure 9(a) displays the results of a 41-layer parametrized tight-binding calculation for Fe(100).[12] Corresponding results obtained from an *ab initio* self-consistent calculation applied to a seven-layer film are shown in Fig. 9(b).[10] Surface states, which are indicated by dots in the figure lie in gaps of the projected bulk bands. Comparison of Figs. 8 and 9 shows that our bulk-band projections produce the same gaps predicted by the thin-film calculations.

There are three prominent gaps in the calculated even-symmetry bands along the $\bar{\Sigma}$ direction for both majority and minority spins, and surface states are predicted in each of these gaps. One of the prominent gaps in the minority-spin complex lies above E_F. Both calculations

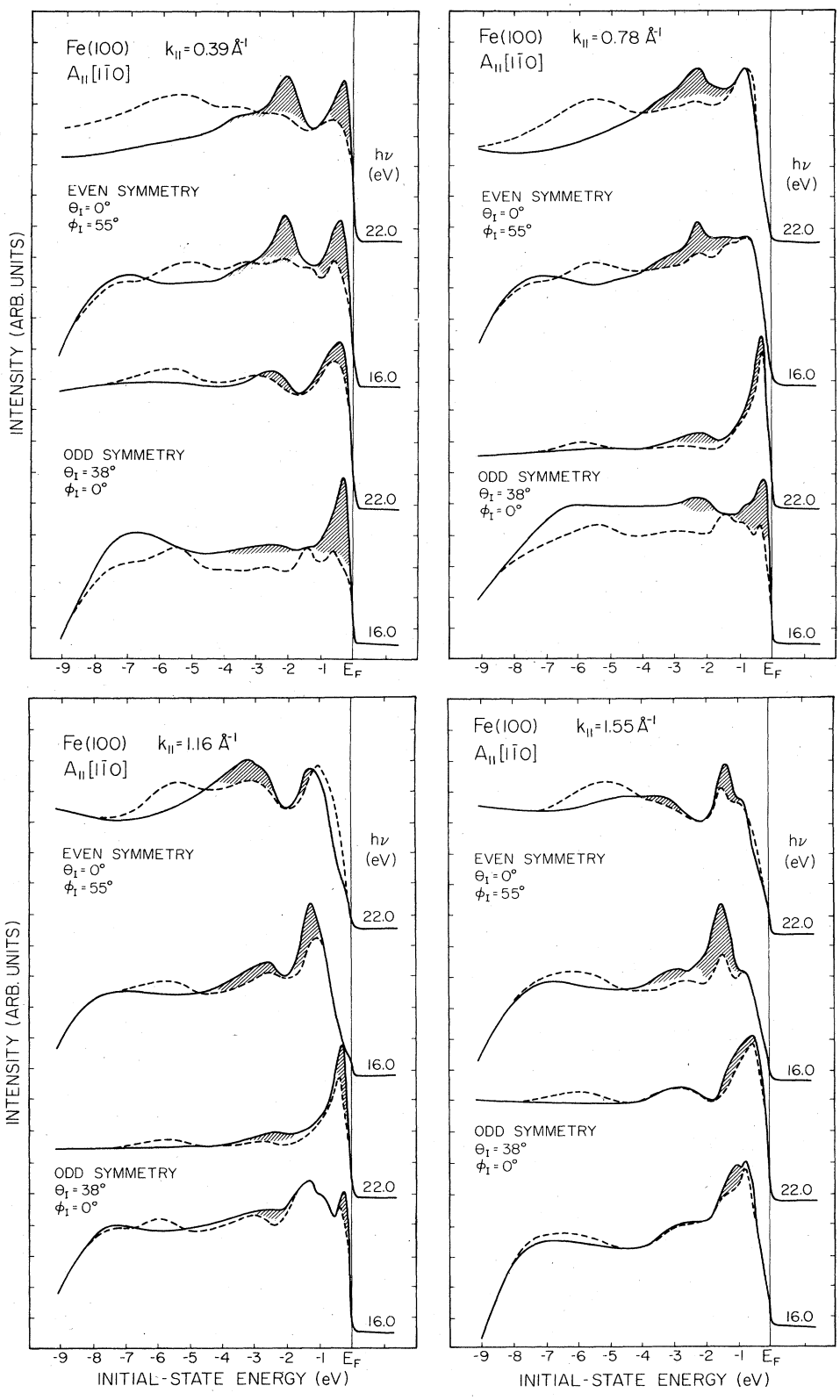

FIG. 6. Off-normal-emission EDC's for both even- and odd-symmetry geometries. Solid lines, clean surface; dashed lines, after 0.3 L oxygen dose. Hatched regions are from surface states. Values of $\vec{k}_{\parallel}$ correspond to $\vec{k}$ values along the $\bar{\Sigma}$ line measured from $\bar{\Gamma}$.

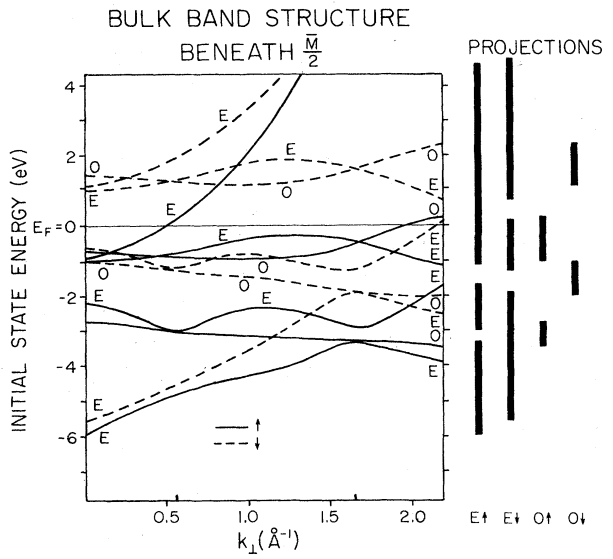

FIG. 7. Intermediate step in bulk-band projection. Left-hand panel: bulk energy bands of Fe along the rod at $\vec{k}_{\|}=0.78$ Å^{-1}, a point half the distance between $\bar{\Gamma}$ and $\bar{M}$ along the $\bar{\Sigma}$ line. Right-hand panel: projections of the even- (E) and odd- (O) symmetry majority (↑) and minority-spin bands (↓) at $\vec{k}_{\|}=0.78$ Å^{-1}.

indicate that a pair of exchange-split, even-symmetry surface states should lie in the majority- and minority-spin gaps which start at $\bar{\Gamma}$ and extend to near the center of the zone along $\bar{\Sigma}$ where the gap is pinched off. The self-consistent calculation predicts binding energies at $\bar{\Gamma}$ for these states to be $\bar{\Sigma}_{1\uparrow}(\vec{k}_{\|}=0)=-4.4$ eV and $\Sigma_{1\downarrow}(\vec{k}_{\|}=0)=-3.2$ eV, and also predicts weak dispersion to lower binding energies as $\vec{k}_{\|}$ increases along $\bar{\Sigma}$. Our experimental data indicate a pair of $\bar{\Sigma}_1$-symmetry surface bands which have binding energies at $\bar{\Gamma}$ of (-3.8 ± 0.2) and (-2.5 ± 0.2) eV, and which exhibit weak energy dispersion to lower binding energies along $\bar{\Sigma}$. We assign these features to the predicted $\bar{\Sigma}_1$-symmetry surface states. These states are predicted to disperse downward by the parametrized calculation, suggesting that the surface bands are pushed down from the continuum above the gap.

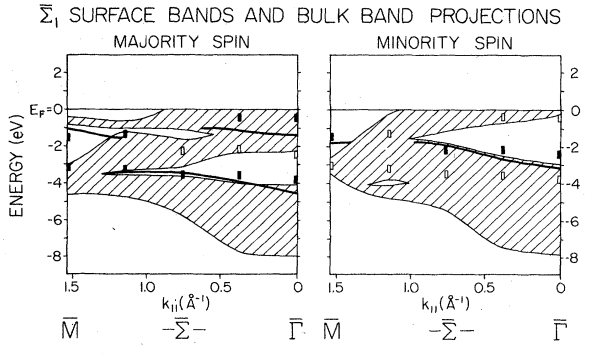

FIG. 8. Projected even-symmetry ($\bar{\Sigma}_1$) bulk bands along $\bar{\Sigma}$ (hatched regions). Solid lines, calculated surface states (Ref. 10). Rectangular points, experimental results. Solid points, assigned to surface states in the panel; open points, assigned to surface states in the other (opposite-spin) panel.

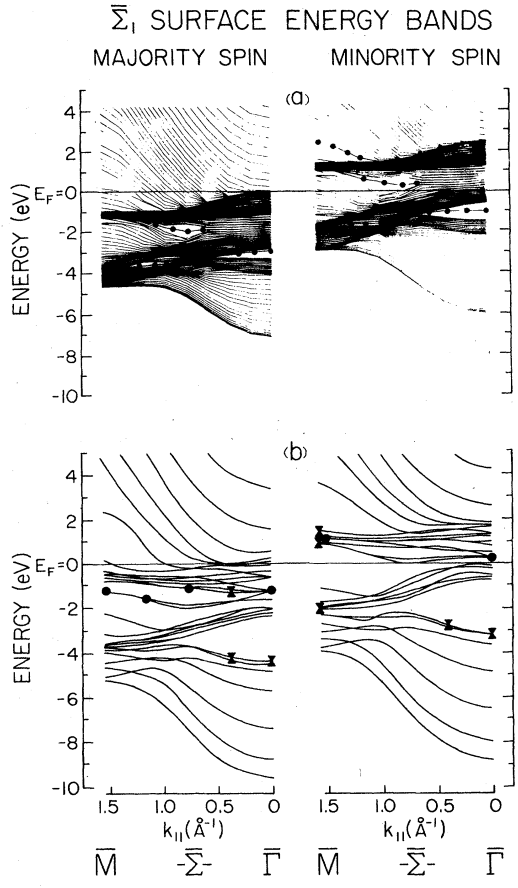

FIG. 9. Calculated even-symmetry ($\bar{\Sigma}_1$) surface bands. (a) 41-layer parametrized calculation (Ref. 12); (b) seven-layer self-consistent calculation (Ref. 10). Dots identify bands having over 80% of their charge in the top layer.

The self-consistent calculations also predict a strong resonance at a binding energy of about -1.0 eV which extends from $\bar{\Gamma}$ to the zone center along the $\bar{\Sigma}$ line in the majority-spin band. The calculated binding energy of this band at $\bar{\Gamma}$ is about -1.0 eV, and a small decrease in binding energy along $\bar{\Sigma}$ is predicted. We observe evidence of a $\bar{\Sigma}_1$-symmetry state near the Fermi level with similar dispersion characteristics along the $\bar{\Sigma}$ direction. Near $\bar{M}$, both parametrized and self-consistent calculations indicate the presence of a majority-spin $\bar{\Sigma}_1$-symmetry surface state. The self-consistent calculations show the state starting at $\bar{M}$ with a binding energy of about -1.0 eV, whereas the parametrized calculation shows the state to be pinched off at $\bar{M}$ and at $\vec{k}_{\|}=0.5$ Å^{-1}. Our experimental data indicate a surface state at $\bar{M}$ with a binding energy of (-1.2 ± 0.2) eV. The state can be seen in the data at

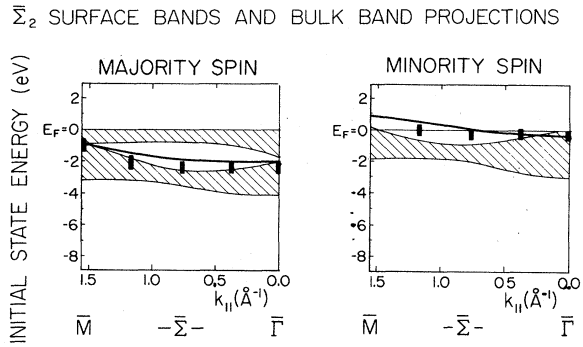

FIG. 10. Projected odd-symmetry ($\bar{\Sigma}_2$) bulk bands along $\bar{\Sigma}$ (hatched regions). Solid lines, calculated surface states (Ref. 10). Rectangular points, experimental results. Peaks corresponding to the two spin subbands have been plotted only on the "assumed" correct panel. The experiments do not discriminate directly between spin.

$\vec{k}_{||}=1.16$ Å^{-1} at the same binding energy. At $\bar{M}$ we also find evidence of a $\bar{\Sigma}_1$-symmetry resonance with a binding energy of (-3.2 ± 0.2) eV. This state appears to be connected with the $\Sigma_{1\uparrow}$ band, which extends to $\bar{\Gamma}$.

We have already reported experimental data and discussed the Σ_2-symmetry surface states.[28] Here, we do not present the photoemission data, but we do include, for completeness, Fig. 10, which illustrates the odd-symmetry $\bar{\Sigma}_2$ bands projected onto the two-dimensional Brillouin zone. We chose to report this example separately because it presented a fairly clear case of a pair of exchange-split surface state bands. Comparison of the experimental results with the calculated surface states[10–12] reveals that there is very convincing agreement in this case. It is interesting to note that the exchange splitting of the $\bar{\Sigma}_2$-symmetry surface states (2.3 eV) is larger than the average bulk magnetic exchange splitting, as predicted theoretically. The self-consistent calculation predicts the $\bar{\Sigma}_2$-band exchange splitting at $\vec{k}_{||}=0.78$ Å to be 2.4 eV, in excellent agreement with our results. The predicted $\bar{\Sigma}_1$-band exchange splitting near $\bar{\Gamma}$ is about 1.3 eV. Our experimental data suggest that the $\bar{\Sigma}_1$ splitting at $\bar{\Gamma}$ is 1.3 eV, but the binding energies measured from E_F are smaller at $\bar{\Gamma}$ by a significant amount (about 20%).

B. The $\bar{\Delta}$ line

Surface states and resonances were investigated along the $\bar{\Delta}$ line using the same two configurations as described in the preceding subsection. Odd-symmetry states ($\bar{\Delta}_2$ symmetry) were probed with pure s-polarized light with $\vec{A}$ along the [010] direction, and electrons were detected in a plane perpendicular to the polarization. Even-symmetry states ($\bar{\Delta}_1$ symmetry) were probed with $\vec{A}$ in the plane of polarization and plane of incidence.

Figure 11 displays EDC's for odd-symmetry configurations at the center of the two-dimensional Brillouin zone for four photon energies. As one might expect, they are very similar to the corresponding results for odd-symmetry results for $\vec{A}$ along the [1$\bar{1}$0] plane. The same

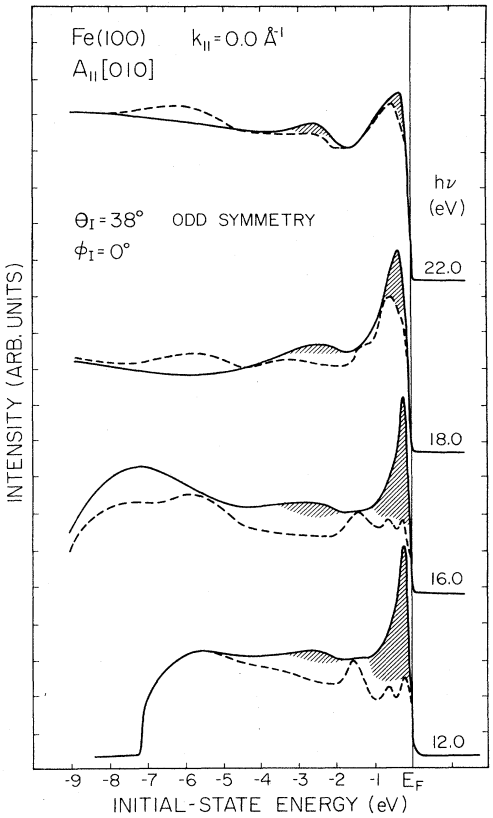

FIG. 11. Normal-emission EDC's taken in odd-symmetry geometry. Solid lines, clean surface; dashed lines, after 0.3 L oxygen dose. Hatched regions are from surface-state emission.

even- and odd-symmetry surface-sensitive features are observed at the zone center, and the EDC's again show that the peaks do not disperse with photon energy, as required for a two-dimensional state. As in the previous EDC's, the solid lines represent clean-surface data and the dashed lines illustrate the effect of adsorption of 0.3 L of oxygen. A small amount of surface oxygen quenches the surface states and allows one to investigate the bulk band structure. Peaks in EDC's shown as dotted lines in Fig. 11 (and Figs. 4 and 5) correspond to bulk transitions from initial states along the Δ line of the three-dimensional Brillouin zone.

Figure 12 displays EDC's for odd- and even-symmetry configurations at four points along the $\bar{\Delta}$ line. We have again displayed EDC's corresponding to both odd- and even-symmetry geometry at each value of $\vec{k}_{||}$, and have also included two photon energies for each symmetry and value of $\vec{k}_{||}$. Comparison of Fig. 6 with Fig. 12 reveals that the spectra differ considerably along the $\bar{\Sigma}$ and $\bar{\Delta}$ directions away from $\bar{\Gamma}$. Although the clean spectra for some photon energies and some values of $\vec{k}_{||}$ exhibit small features which may reflect an underlying bulk initial state, there is, in general, very little evidence of significant contributions to the clean-surface EDC's (in the photon range used here) from bulk states. The EDC's at each value of $\vec{k}_{||}$ exhibit strong differences between even- and odd-symmetry pairs and strong similarities between pairs

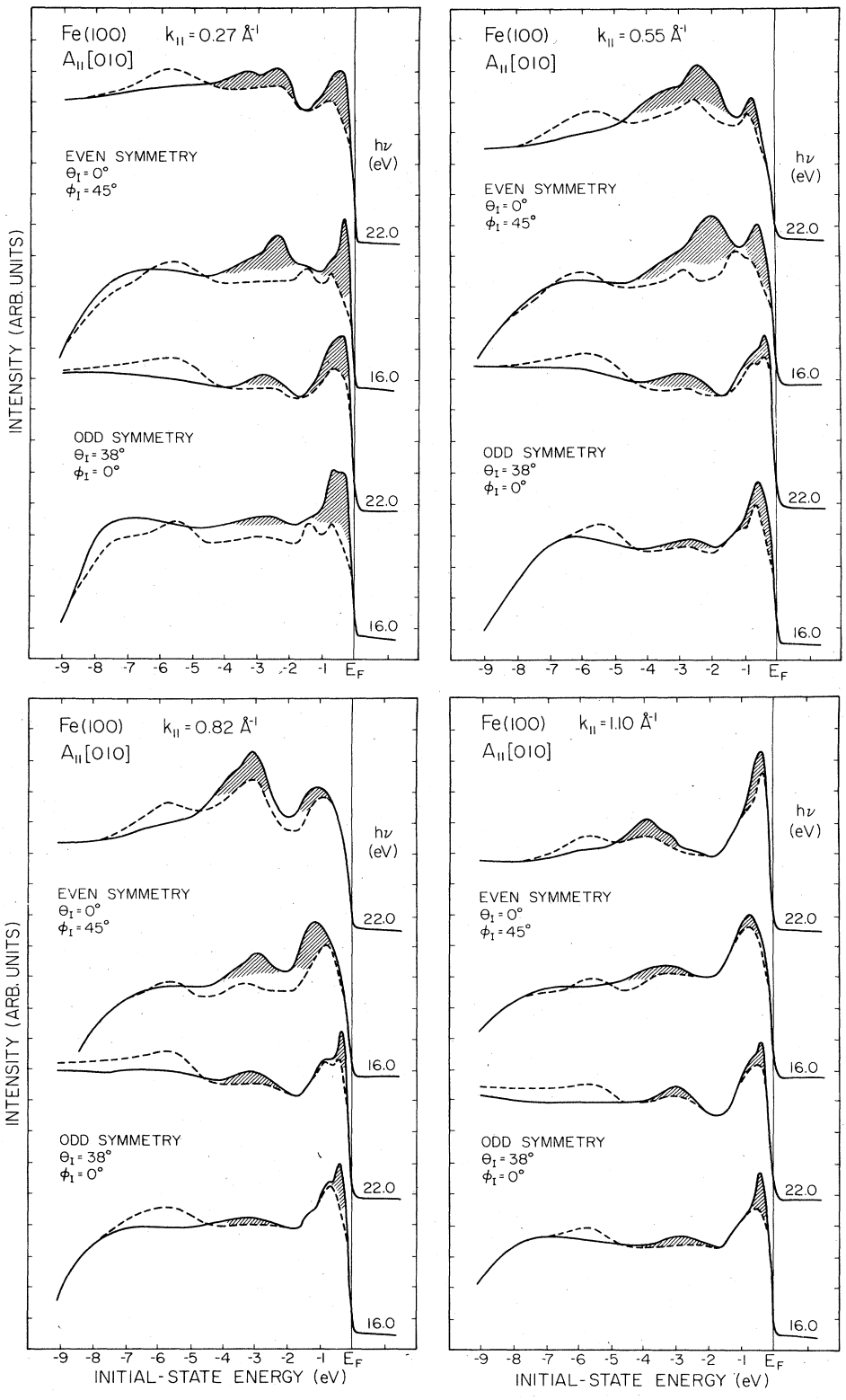

FIG. 12. Off-normal-emission EDC's for both even- and odd-symmetry geometries. Solid lines, clean surface; dashed lines, after 0.3 L oxygen dose. Hatched regions are from surface states. Values of $\vec{k}_{\parallel}$ correspond to $\vec{k}$ along the $\bar{\Delta}$ line measured from $\bar{\Gamma}$.

corresponding to a given symmetry and different photon energies. It is interesting to note here that an exposure of 0.3 L of oxygen was found to have very little effect on EDC's obtained from the Fe(110) surface over a wide photon-energy range (10—30 eV). The reason for this is that there is an allowed even-symmetry final-state band along the $\bar{\Sigma}$ direction of the three-dimensional Brillouin zone. As expected, photoemission spectra obtained from clean Fe(110) surfaces were found to be dominated by bulk interband transitions. The (110) surface turns out to be the best surface for mapping the bulk band structure of Fe.

Figure 13 displays the band structure of Δ_2-symmetry bulk states of Fe projected along the $\bar{\Delta}$ line of the two-dimensional Brillouin zone. As in the preceding subsection, we have projected the even- and odd-symmetry states separately to facilitate plotting the results of our experiments. The $\bar{\Delta}_2$-symmetry bands are not particularly interesting. There is a single gap at $\bar{X}$ in the majority-spin bands about 2 eV below E_F, and the gap is pinched off abruptly away from $\bar{X}$ along the $\bar{\Delta}$ direction. This gap lies above E_F in the minority-spin bands. Our experimental data show strong evidence of surface states near $\bar{\Gamma}$, and, as shown in Fig. 12, there is good evidence of a $\bar{\Delta}_2$-symmetry surface resonance along the $\bar{\Delta}$ direction near E_F, and a weak $\bar{\Delta}_2$-symmetry surface state which appears at binding energies between -2.5 and -3.2 eV. It is possible that the state with the higher binding energy is a majority-spin surface state pushed out from the bottom of the bulk-band continuum, and that the other state is the corresponding minority-spin surface state which becomes a resonance away from $\bar{\Gamma}_1$. These $\bar{\Delta}_2$ surface resonances appear to have been predicted by slab calculations.[11] The exchange-split $\bar{\Delta}_2$ resonances displayed in Fig. 3 of Ref. 11 exhibit rather nice agreement with the data shown in Fig. 13.

Figure 14 displays the Δ_1-symmetry bulk bands projected onto the $\bar{\Delta}$ line with points corresponding to our experimental data. There are a number of predicted $\bar{\Delta}_1$ (even-symmetry) surface states.[10–12] Both majority- and minority-spin Δ_1 bands exhibit gaps which contain surface states. The prominent gap which starts at $\bar{X}$ and is pinched off at about half the distance to the zone center lies completely below E_F for both majority- and minority-spin bands. The parametrized calculation[12] predicts the binding energies of $\bar{\Delta}_{1\uparrow}$ and $\bar{\Delta}_{1\downarrow}$ bands at $\bar{X}$ to be approximately -3.3 and -1.8 eV; the self-consistent calculation yields -4.8 and -3.5 eV for these states. Both calculations indicate a slight decrease in binding energy of these states along the $\bar{\Delta}$ line toward $\bar{\Gamma}$. Our experimental data exhibit a pair of surface-sensitive $\bar{\Delta}_1$-symmetry peaks with binding energies at $\bar{X}$ of (-4.0 ± 0.2) and (-3.1 ± 0.2) eV. These peaks can be seen from $\bar{X}$ to extend over at least half the distance to $\bar{\Gamma}$, and their binding energies decrease away from $\bar{X}$. We assign these peaks to the $\bar{\Delta}_{1\uparrow}$ and $\bar{\Delta}_{1\downarrow}$ surface states. They appear to become resonances at about half the distance to $\bar{\Gamma}$ along $\bar{\Delta}$.

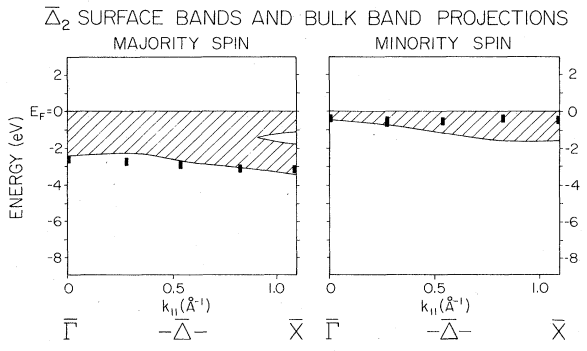

FIG. 13. Projected odd-symmetry ($\bar{\Delta}_2$) bulk bands along $\bar{\Delta}$ (hatched regions). Rectangular points, experimental results. Peaks corresponding to the two spin subbands have been plotted only on the "assumed" correct panel.

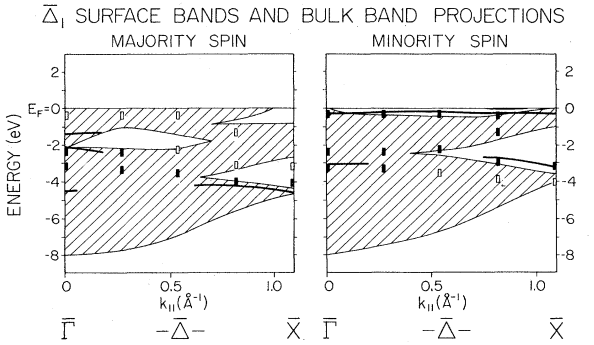

FIG. 14. Projected even-symmetry ($\bar{\Delta}_1$) bulk bands along $\bar{\Delta}$ (hatched regions). Solid lines, calculated surface states (Ref. 10). Rectangular points, experimental results. Solid points, assigned to surface states in the panel; open points, assigned to surface states in the other (opposite-spin) panel.

The calculations also predict a minority-spin $\bar{\Delta}_1$ surface state very near E_F which extends over most of the $\bar{\Delta}_1$ line. The self-consistent calculations[10,11] show this state extending over most of the $\bar{\Delta}$ line, and also show a splitting of the band near $\bar{X}$. The parametrized calculation[12] shows this state passing above E_F at $\vec{k}_{||}\simeq0.5$ Å^{-1}. No significant occupied $\bar{\Delta}_1$-symmetry surface states are predicted to lie near E_F in the majority-spin band by either calculation. Our experimental data exhibit a strong $\bar{\Delta}_1$-symmetry surface-state peak near E_F which extends from $\bar{\Gamma}$ to $\bar{X}$. The structure is considerably broader and shifted at $\vec{k}_{||}=0.82$ Å^{-1}, suggesting that it splits near $\bar{X}$, as shown by the self-consistent calculation. We assign the $\bar{\Delta}_1$-symmetry peaks near E_F to the minority-spin band predicted by the calculations.

The $\bar{\Delta}_1$-symmetry surface-sensitive peaks near $\bar{\Gamma}$ remain to be accounted for. The slab calculations and our projection of the bulk majority-spin $\bar{\Delta}_1$-symmetry bands show that a gap opens up, starting at $\bar{\Gamma}$, which extends over half the distance to $\bar{X}$. All three slab calculations show a majority-spin surface state in this gap. The self-consistent calculations also suggest a strong surface resonance extending from $\bar{\Gamma}$ to the gap which opens up at

$\vec{k}_{||} \approx 0.5$ Å^{-1} in the majority-spin band. Our experimental data exhibit two peaks which could account for this surface state and the resonance. The binding energy of the peak nearest E_F at $\bar{\Gamma}$ is (-2.2 ± 0.2) eV, and the peak has the same binding energy at $\vec{k}_{||} = 0.27$ Å^{-1}. Halfway to the zone edge, this surface state is pinched off, and has nearly the same binding energy as the minority-spin $\bar{\Delta}_1$ surface state in a different gap, one which starts at $\bar{X}$. Our experiment does not resolve spin, but if this interpretation is correct, the spin polarization associated with the middle surface-sensitive peak should change sign near $\vec{k}_{||} = 0.5$ Å^{-1}. The $\bar{\Delta}_1$-symmetry peak at $\bar{\Gamma}$ with binding energy of -3.2 eV is most likely to be associated with the predicted surface resonance in the majority-spin band.

C. The $\bar{Y}$ line

The third high-symmetry line in the two-dimensional Brillouin zone is the $\bar{Y}$ line. Planes in the three-dimensional Brillouin zone which intersect the $\bar{Y}$ line do not have inversion symmetry; therefore, only the two-dimensional surface bands will be even or odd in this plane. The bulk bands are not separable into even and odd components. When mapping the surface electronic structure along the [100] and [110] directions, $\vec{k}_{||}$ was changed by changing only the angle θ. However, to probe $\vec{k}_{||}$ along the $\bar{Y}$ line both θ and ϕ must be adjusted. The ability to rotate our analyzer about two independent axes allowed us to easily adjust $\vec{k}_{||}$ so that the desired point along $\bar{Y}$ was probed.

Our experiments which probed the $\bar{Y}$ line were performed with $\vec{A}$ along the [100] direction so that s- and p-polarization configurations did not correspond to pure odd-state or pure even-state symmetry. Therefore, along $\bar{Y}$, we not only failed to discriminate between the two spins, but we also did not separate even- and odd-symmetry states. However, we were able to identify some surface states along the $\bar{Y}$ direction. Because the plane containing the $\bar{Y}$ line is not a symmetry plane of the three-dimensional Brillouin zone, the bulk projections shown in Fig. 15 include all bands which are projected onto the $\bar{Y}$ line. Also shown in Fig. 15 are the surface-sensitive bands from EDC's (not shown) and the surface-state bands from the self-consistent calculation. The solid lines represent even symmetry $\bar{Y}_1$ surface bands and the dashed lines represent the odd-symmetry $\bar{Y}_2$ surface bands.

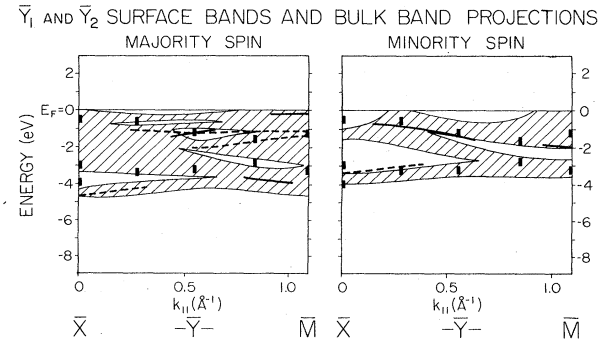

FIG. 15. Projected even- and odd-symmetry bulk bands along $\bar{Y}$ (hatched region). Rectangular points, experimental results.

There are several absolute gaps in both the majority- and minority-spin projections shown in Fig. 15 and which are also evident in the slab calculations.[10–12] By "absolute gaps" we mean that these gaps do not depend on symmetry, but rather are gaps present after projecting all bands of a given spin. A gap opens up in the majority-spin bands at $\bar{X}$ centered around a binding energy of -3.8 eV, and a much larger minority-spin gap is seen at $\bar{X}$ centered around -2.5 eV. In this energy region we see two surface-sensitive peaks at $\bar{X}$. These peaks lie within the gaps at $\bar{X}$ and can be attributed to the predicted $\bar{Y}_2$-symmetry surface states. Considering points along $\bar{Y}$ toward $\bar{M}$, only one peak is observed in the vicinity of these gaps. Perhaps the majority and minority-spin components can no longer be resolved, and only one peak is observed with a binding energy equal to the average for the two surface states.

The next gap seen as one considers higher energy is the gap present at $\bar{M}$ at -2.4 eV in the minority-spin bands and which opens up just past $\bar{M}$ at -3.0 eV in the majority-spin bands. There are two surface bands in this region: the lower band lies within the majority-spin gap, but the upper band lies just above the minority-spin gap. The parametrized calculation predicts both an odd- and even-symmetry surface state in this gap, but the self-consistent calculation,[10] which does not clearly show this gap, predicts only an even-symmetry surface state in this region. One other surface band was observed, one which begins at $\bar{X}$ at -0.5 eV binding energy and disperses downward along the $\bar{Y}$ direction toward $\bar{M}$. There are two gaps in this region in both the majority- and minority-spin projections. Even- and odd-symmetry majority-spin surface states and even-symmetry minority-spin surface states are predicted in these gaps by both calculations. Owing to the inability of our experiments to distinguish symmetries in the experimental configuration used in this particular case, and the complexity of the observed and predicted surface bands, we cannot make unambiguous assignments for these peaks, and, indeed, for most of the bands along $\bar{Y}$. Because the $\bar{Y}$ line has more surface bands than either the $\bar{\Sigma}$ or $\bar{\Delta}$ lines, and because there are substantial differences in the surface states predicted by the two calculations, a reexamination of this region with polarized light and a geometry which would distinguish symmetry would be quite interesting.

V. DISCUSSION

We have presented a comprehensive set of photoemission data and bulk energy-band projections which permit us to identify surface states and surface resonances along three high-symmetry lines of the two-dimensional Brillouin zone of Fe(100). Our studies of these states along the $\bar{\Delta}$ and $\bar{\Sigma}$ lines were carried out in configurations which permitted discrimination between even and odd symmetry, and comparison of the surface-state dispersion of pairs of surface states with accurate parametrized and *ab initio* self-consistent calculations has permitted us to assign some of the surface-state bands to exchange-split

minority- and majority-spin surface-state bands.

The overall agreement between our experimentally determined surface bands and those predicted by slab calculations is, in general, quite good. It is at least clear from our results that in nearly every case where both the self-consistent and parametrized calculations predicted prominent surface states or surface resonances, surface-sensitive features in the photoemission spectra were observed. In addition, in most cases, the features were found to have the correct symmetry and to exhibit the predicted dispersion with $\vec{k}_{||}$. In most cases, the self-consistent calculations yield the more accurate binding energies. There are several cases where assignment of the structure in photoemission data to surface states appears to be unambiguous. In these cases, the symmetry, binding energies, and exchange splitting have been compared directly with calculated results with very encouraging results.

Perhaps the clearest case of excellent agreement is the exchange-split $\bar{\Sigma}_2$ bands. This appears to be a classic example of a Shockley surface state. The exchange splitting of the $\bar{\Sigma}_2$ surface-state bands at $\vec{k}_{||}=0.78$ Å^{-1} is 2.3 eV, in excellent agreement with the calculated self-consistent surface-state exchange splitting at the same point (2.4 eV). The corresponding parametrized-calculation value of 2.0 eV is significantly lower. The exchange splitting of the $\bar{\Sigma}_2$ surface-state bands averaged over the $\bar{\Sigma}$ line is approximately 2.3 eV. The calculated bulk exchange splitting varies from 1.3 eV near the bottom of the band to 2.2 eV near the top, and our results, presented elsewhere,[20] support these predictions. Thus the surface exchange splitting is larger than the averaged bulk value for ferromagnetic Fe.

A second case where a pair of bands can be assigned with reasonable certainty to exchange-split surface states occurs along the $\bar{\Delta}$ line near $\bar{X}$. A pair of $\bar{\Delta}_1$-symmetry surface states are observed to originate at $\bar{X}$ and extend to a point halfway to $\bar{\Gamma}$, where the gaps pinch off. The exchange splitting of these bands is approximately 1.2 eV, which is considerably smaller than that of the $\bar{\Sigma}_2$ states, and also slightly smaller than the value predicted by the self-consistent calculation (2.4 eV). The predicted[11] exchange-split $\bar{\Delta}_2$ resonances also appear to agree nicely with our experimental data.

Transition-metal surface states are extremely sensitive to both the surface and bulk potentials.[12] Small shifts in the bulk potential can create or destroy Shockley surface states, and small changes in the surface potential can create surface states (Tamm states) and destroy Shockley states. The parametrized calculations involve a restricted tight-binding basis set for the surface basis functions, and shifts are required in the surface potential to force the inadequate basis set to yield surface-layer charge neutrality. Our recent experimental work has shown that the calculated bulk bands of Fe are accurate. This indicates the bulk energy eigenvalues used to obtain the slab-calculation parameters were also accurate. Our surface experiments therefore test how accurately the surface parameters are determined by requiring charge neutrality.

Tables I and II summarize binding energies of surface states identified by our experiments in comparison with calculated values based on parametrized[12] and self-consistent[10,11] techniques. We have included in the tables only surface states which we have been able to apply symmetry tests to, and in which we have a fairly high degree of confidence in the assignment. This paper intentionally presents a large amount of experimental data so that the reader may judge for himself the strength of our assignments. Clearly, a detailed comparison between the various results is not justified. However, one can argue, based on the results contained in these tables and shown in the corresponding figures, that all of the calculations yield reasonably good accounts of the observed surface states. The self-consistent calculations yield better overall agreement for surface-state binding energies and exchange splitting throughout the two-dimensional Brillouin zone. The parametrized calculations (41 layers) yield a much higher density of bands, which permits easy identification

TABLE I. Measured and calculated binding energies of $\bar{\Sigma}$ surface states at various points of the two-dimensional Brillouin zone.

Spin $\vec{k}_{||}$ (Å^{-1})	Experiment	Self-consistent calculation[a]	Self-consistent calculation[b]	Parametrized calculation[c]
		$\bar{\Sigma}_2$ symmetry		
↑ 0.0 ($\bar{\Gamma}$)	2.6	2.5	2.2	2.6
↓ 0.0 ($\bar{\Gamma}$)	0.2	0.1	0.3	0.4
↑ 0.78	2.5	2.6	2.4	2.2
↓ 0.78	0.2			
↑ 1.55 ($\bar{M}$)	1.0	1.3	1.0	1.0
		$\bar{\Sigma}_1$ symmetry		
↑ 0.0 ($\bar{\Gamma}$)	3.8	4.3	4.4	2.8
↓ 0.0 ($\bar{\Gamma}$)	2.4	2.5	3.2	1.0
↑ 0.78	3.5	3.5	3.8	3.6
↓ 0.78	2.2	1.8	2.4	1.4
↑ 1.55 ($\bar{M}$)	3.2	3.5	1.8	3.8
↓ 1.55 ($\bar{M}$)	1.4	1.5	1.1	1.8

[a]Reference 10. [b]Reference 11. [c]Reference 12.

TABLE II. Measured and calculated binding energies of $\bar{\Delta}$ surface states at various points of the two-dimensional Brillouin zone; * indicates that other surface states or surface resonances are predicted and that the binding-energy assignment may not be unambiguous.

Spin $\vec{k}_{\parallel}$ (Å^{-1})	Experiment	Self-consistent calculation[a]	Self-consistent calculation[b]	Parametrized calculation[c]
		$\bar{\Delta}_2$ symmetry		
↑ 0.0 ($\bar{\Gamma}$)	2.7	2.5		
↓ 0.0 ($\bar{\Gamma}$)	0.3	0.2		
↑ 0.55	2.8	2.8		
↓ 0.55	0.5	0.5		
↑ 1.10 ($\bar{X}$)	3.2	3.0		
↓ 1.10 ($\bar{X}$)	0.5	0.8		
		$\bar{\Delta}_2$ symmetry		
↑ 0.0 ($\bar{\Gamma}$)	2.3	2.5*	2.2	2.4
↓ 0.0 ($\bar{\Gamma}$)	0.2	0.2	0.4	0.4
↑ 0.53	2.2	2.5*	2.2	2.0
↓ 0.55	0.2	0.2*	0.3	
↑ 1.10 ($\bar{X}$)	4.0	4.2	4.7	3.5
↓ 1.10 ($\bar{X}$)	3.2	2.8	3.7	1.8

[a]Reference 10. [b]Reference 11. [c]Reference 12.

of the gaps in relation to the projected bulk band structure.

Our study of surface electronic properties of Fe is based on the (100) crystal face. We have conducted extensive work on Fe(110) surfaces and some work on the Fe(111) surface. We were able to clean the Fe(110) surface to a point where O, S, and C contamination were comparable to the concentrations ($\frac{1}{10}$ ML) required to observe surface states on Fe(100). We did observe some sensitivity of photoemission peaks on the (110) and (111) surfaces; however, the effects were small in comparison to what is shown by the EDC's for Fe(100) in the photon-energy range studied in this paper. Most of the structure in EDC's obtained from clean (111) and (110) surfaces could be accounted for in terms of bulk states.[20] Emission along the high-symmetry line (normal emission) for the (110) and (111) surfaces is dominated by bulk transitions because there is an appropriate (even-) symmetry final-state band.[20]

ACKNOWLEDGMENTS

We are pleased to thank the staff of the Synchrotron Radiation Center, Stoughton, Wisconsin, for their assistance. The work was supported by the National Science Foundation (NSF) (Grants No. DMR-79-23629 and DMR-83-04368) and the Robert A. Welch Foundation. The Synchrotron Radiation Center is supported by the NSF.

[1]J. Callaway and C. S. Wang, Phys. Rev. B **16**, 2095 (1977).
[2]H. S. Greenside and M. A. Schlüter, Phys. Rev. B **27**, 3111 (1983).
[3]V. L. Moruzzi, J. F. Janak, and A. R. Williams, *Calculated Electronic Properties of Metals* (Pergamon, New York, 1978).
[4]C. S. Wang and J. Callaway, Phys. Rev. B **15**, 298 (1977).
[5]J. R. Anderson, D. A. Papaconstantopoulous, L. L. Boyer, and J. E. Schirber, Phys. Rev. B **20**, 3172 (1979).
[6]F. Weling and J. Callaway, Phys. Rev. B **26**, 710 (1983).
[7]D. G. Dempsey, W. R. Grise, and L. Kleinman, Phys. Rev. B **18**, 1270 (1978); **18**, 1550 (1978); F. J. Arlinghans, J. G. Gay, and J. R. Smith, *ibid.* **21**, 2055 (1980).
[8]C. S. Wang and A. J. Freeman, Phys. Rev. B **19**, 793 (1979); **21**, 4585 (1980).
[9]H. Krakauer, A. J. Freeman, and E. Wimmer, Phys. Rev. B **28**, 610 (1983); O. Jepsen, J. Madsen, and O. K. Andersen, *ibid.* **26**, 2790 (1982).
[10]C. S. Wang and A. J. Freeman, Phys. Rev. B **24**, 4364 (1981).
[11]S. Ohnishi, A. J. Freeman, and M. Weinert, Phys. Rev. B **28**, 6741 (1983).
[12]D. G. Dempsey, L. Kleinman, and E. Caruthers, Phys. Rev. B **12**, 2932 (1975); **13**, 1489 (1976).
[13]D. G. Dempsey and L. Kleinman, Phys. Rev. Lett. **39**, 1297 (1977).
[14]L. N. Liebermann, J. Clinton, D. M. Edwards, and J. Mathon, Phys. Rev. Lett. **25**, 232 (1970).
[15]L. N. Liebermann, D. R. Fredkin, and H. B. Shore, Phys. Rev. Lett. **22**, 539 (1969).
[16]E. Kisker, J. Phys. Chem. **87**, 3597 (1983).
[17]R. Feder, W. Gudat, E. Kisker, R. Rodriguez, and K. Schröder, Solid State Commun. **46**, 619 (1983).
[18]G. Treglia, F. Ducastelle, and P. Spanjaard, J. Phys. **43**, 341 (1982).
[19]A. Liebsch, Phys. Rev. Lett. **43**, 1431 (1979).
[20]A. M. Turner, A. W. Donoho, and J. L. Erskine, Phys. Rev. B **29**, 2986 (1984).

[21]H. A. Stevens, A. W. Donoho, A. M. Turner, and J. L. Erskine, J. Electron. Spectrosc. Relat. Phenom. **32**, 327 (1983).
[22]G. K. Ovrebo and J. L. Erskine, J. Electron. Spectrosc. Relat. Phenom. **24**, 189 (1981).
[23]A. M. Turner, Yu-Jeng Chang, and J. L. Erskine, Phys. Rev. Lett. **48**, 348 (1982).
[24]T.-C. Chiang, J. A. Knapp, M. Aono, and D. E. Eastman, Phys. Rev. B **21**, 3513 (1980).
[25]W. Eberhard and E. W. Plummer, Phys. Rev. B **21**, 3245 (1980).
[26]J. Hermanson, Solid State Commun. **22**, 9 (1977).
[27]W. Eberhard and F. J. Himpsel, Phys. Rev. B **21**, 5572 (1980).
[28]A. M. Turner and J. L. Erskine, Phys. Rev. B **28**, 5628 (1983).